Eur. J. Mineral.
Fast Track DOI: 10.1127/0935-1221/2008/0020-1836

Fast Track Article

The $P2_1/m$ - $C2/m$ phase transition in synthetic amphiboles in the system Li_2O-Na_2O-MgO-SiO_2-H_2O: an high-T FTIR study

Giancarlo Della VENTURA[1,4], Fabio BELLATRECCIA[1], Gianluca IEZZI[2,3,*], Roberta OBERTI[4] and Fernando CÁMARA[4]

[1] Dipartimento di Scienze Geologiche, Università Roma Tre, Largo S. Leonardo Murialdo 1, 00146, Roma, Italy
*Corresponding author, e-mail: dellaven@uniroma3.it
[2] Dipartimento di Scienze della Terra, Università "G. D'Annunzio", 66013 Chieti Scalo, Italy
[3] Department of Seismology and Tectonophysics, Istituto Nazionale di Geofisica e Vulcanologia, Roma, 00100 Italy
[4] CNR-Istituto di Geoscienze e Georisorse, unità di Pavia, via Ferrata 1, 27100 Pavia, Italy

Abstract: The $P2_1/m \leftrightarrow C2/m$ phase-transition has been studied by high-T FTIR analysis on a series of synthetic amphiboles in the Li_2O–Na_2O–MgO–SiO_2–H_2O (LNMSH) system. Spectra were collected in the T range 25–450 °C on KBr disks. All examined amphiboles have $P2_1/m$ symmetry at room T. Their OH-stretching FTIR spectrum consists of two main bands at ~ 3740 and 3715 cm^{-1}. At the transition temperature (T_c), these bands merge into one single absorption centred at ~ 3720 cm^{-1}, and no further change is observed beyond this T. Significant modifications consisting in peak shifting and band broadening are also observed in the MIR (medium infrared) 1300–640 cm^{-1} region. T_c values for the different compositions were estimated based on various methods; the most reliable procedure is considered to be the fit of Landau 2-4-6 potentials using band shifts observed in the MIR region. The T_c values obtained for all samples are consistent with previous results obtained on two members of the series examined here by single-crystal or synchrotron powder HT-XRD (high-T X-ray diffraction). They correlate linearly with the aggregate cation radius at $M(6)$ [T_c (°C) = 803–533 $\langle r_{M(6)} \rangle$; $R^2 = 0.97$]. This work thus provide a measure of the role played by the size of the $M(6)$ polyhedron in determining the T_c in simple chemical systems where the B-site occupancy (and geometry) is the only variable. The slope of the equation is far less steep in the LNMSH system than in cummingtonite; crystal-chemical reasons for this behaviour are discussed, and the local order between A and monovalent B cations is suggested to be the major constraint. In more complex systems, inspection of the available data shows that other factors such as the aggregate size of the strip of octahedra must be taken into account.

Key-words: synthetic amphiboles, LNMSH system, HT-FTIR spectroscopy, phase transition.

Introduction

Monoclinic amphiboles with small B cations (Mg, Fe^{2+}) undergo a displacive $P2_1/m \leftrightarrow C2/m$ phase-transition as a function of temperature (T) and/or pressure (P), and the T_c and P_c values depend on composition and/or cation order, which may be followed by the aggregate cation radius at the $M(6)$ site, $\langle r_{M(6)} \rangle$ (Yang & Hirschmann, 1995; Yang & Prewitt, 2000; Boffa Ballaran *et al*., 2000, 2001, 2004). More recently, the same transition behaviour was detected in synthetic amphiboles with 1:1 monovalent and small divalent B cations (*e.g*., ^{B}(NaMg) and ^{B}(LiMg)), and evidences were found that T_c depends on the aggregate cationic radius at both the $M(6)$ and $M(1,2,3)$ sites (Cámara *et al*., 2003a, 2008; Iezzi *et al*., 2004, 2005; Welch *et al*., 2007). Notwithstanding these efforts, a comprehensive P-T-X model for the phase transition in amphiboles still needs to be developed.

Oberti *et al*. (2000) used single-crystal X-ray refinement (SREF), Secondary Ion Mass Spectrometry (SIMS), and Fourier Transform Infrared spectroscopy (FTIR) to show that some synthetic amphiboles obtained by Gibbs *et al*. (1962) and Maresch & Langer (1976) in the Li_2O-Na_2O-MgO-SiO_2-H_2O (LNMSH) system have a very peculiar mixture of B cations ($Mg_{0.97}Li_{0.27}H_{0.12}Na_{0.64}$) and $P2_1/m$ symmetry. This finding prompted a series of experimental studies aimed at characterizing the actual composition and structural features of LNMSH amphiboles under different T, P and X conditions.

Cámara *et al*. (2003a) and Iezzi *et al*. (2004) showed by single-crystal XRD analysis that the Li-free $^{A}Na^{B}_{0.81}(Na_{0.81}Mg_{1.19})\,^{C}Mg^{T}_{5}Si_8O^{W}_{22}(OH)_2$ composition (sample 334) has $P2_1/m$ symmetry at room T, and undergoes a second-order $P2_1/m \leftrightarrow C2/m$ phase transition at T_c = 257 °C. Iezzi *et al*. (2005) found by synchrotron-

* Presently at: Dipartimento di Geotecnologie per l'Ambiente ed il Territorio, Università G.d'Annunzio, Chieti, 66013 Italy.

DOI: 10.1127/0935-1221/2008/0020-1836

0935-1221/08/0020-1836 $ 3.60

radiation XRPD (X-ray powder diffraction) that the stoichiometric ^{A}Na ^{B}(LiMg) $^{C}Mg_5^{T}Si_8O_{22}^{W}(OH)_2$ composition has a T_c of 326 °C. Also, a treatment of the data in the frame of the Landau theory allowed these authors to show that the thermodynamic character of the phase transition is tricritical for this composition. It is thus interesting to check the transition behaviour within the ^{B}Na → ^{B}Li solid solution. Iezzi *et al*. (2006) synthesized a series of terms in this solid solution, and showed by TEM and FTIR that they all have $P2_1/m$ symmetry at room T. In this work, we examine by *in situ* high-T FTIR spectroscopy the complete set of samples of Iezzi *et al*. (2006) with the aim to investigate changes in the T_c of the $P2_1/m \leftrightarrow C2/m$ phase transition. Noteworthy, the LMNSH system does not allow order-disorder phenomena between the $M(6)$ and the $M(1, 2, 3)$ sites (which extensively occur in the presence of Fe^{2+}), and hence can provide unambiguous modelling of the effect of the B cations on the phase-transition behaviour.

FTIR spectroscopy can be used to detect the transition temperature on amphibole powders either from the merging of the two OH absorption bands observed in the $P2_1/m$ symmetry into the unique band observed in the $C2/m$ symmetry or from careful analysis of the spectrum in terms of peak shift and broadening in the MIR region (*e.g.*, Boffa Ballaran *et al*., 2004). Both these methods require extrapolation of the data. In the case of two samples, we were able to test the accuracy of the FTIR-based approach by comparing the extrapolated T_c values with those obtained by single-crystal and powder X-ray diffraction (sample 334: Cámara *et al*., 2003a; sample 407: Iezzi *et al*., 2005, respectively).

Experimental methods

Details on the synthesis and characterization of the amphibole compositions examined here (Table 1) are reported in Iezzi *et al*. (2006). In brief, hydrothermal synthesis using silicate gels as the starting materials was done at 800 °C, 0.4 GPa using an internally heated vessel pressurized with Ar, at the University of Hannover (Germany). Selected-area electron diffraction (SAED) showed all samples to have $P2_1/m$ symmetry at room-T (Iezzi *et al*., 2006).

FTIR spectra were collected on a Nicolet 760 spectrophotometer, equipped with KBr beamsplitter and a DTGS detector. The nominal resolution was 4 cm^{-1} and spectra are the average of 64 scans. Samples were prepared as KBr pellets; two disks were used, one for the OH-stretching region (5 mg of powder in 150 mg KBr) and a second for the MIR (< 1300 cm^{-1}) region (1 mg of powder in 300 mg KBr). *In situ* high-T spectra were collected using a Specac™ P/N 5850 high-T/high-P cell; the temperature was controlled using a Cr-Al thermocouple placed close to the sample and is accurate within ± 1 °C, according to the manufacturer. High-T spectra were collected with a step of 20 °C which was reduced to 10 °C when approaching the T_c predicted on the basis of the work of Cámara *et al*. (2003a) and Iezzi *et al*. (2005); each sample was equilibrated for 15 min at any target T before the FTIR data collection.

Table 1. Sample labels and nominal composition for the amphiboles of this study.

Sample	nominal composition
403	Na (NaMg) Mg_5 Si_8 $O_{22}(OH)_2$
405	Na ($Na_{0.6}Li_{0.4}Mg_1$) Mg_5 Si_8 $O_{22}(OH)_2$
406	Na ($Na_{0.2}Li_{0.8}Mg_1$) Mg_5 Si_8 $O_{22}(OH)_2$
407	Na (LiMg) Mg_5 Si_8 $O_{22}(OH)_2$

Room-*T* OH-stretching FTIR spectra

The room-T OH-stretching infrared spectra of the studied samples have been already discussed by Iezzi *et al*. (2004, 2005, 2006). They consist of two main bands at ~ 3740 and 3715 cm^{-1}, which are assigned to two independent OH groups in the $P2_1/m$ structure, which interact with the strongly off-centred ^{A}Na, as shown by the structure refinement (Iezzi *et al*., 2004). Two minor absorptions in the spectra are centred at 3690 and 3670 cm^{-1}, respectively. These latter bands are assigned to OH groups adjacent to vacant A sites in the structure, and indicate a slight departure from the nominal composition (cummingtonite component, *i.e.* vacancy at the A site locally balanced by excess ^{B}Mg with respect to 1.0 apfu).

High-*T* FTIR spectra: the OH-stretching region

Figure 1 shows the complete set of spectra collected at increasing T on sample 405. The main bands at 3740 and 3715 cm^{-1} gradually merge into a single, broad and symmetric absorption due to the $P2_1/m \rightarrow C2/m$ phase transition. The same kind of behaviour was recorded for all samples, but the merge of the two bands occurs at different temperatures. FTIR analysis also confirms that the transition is reversible and not quenchable; when decreasing the temperature, the OH-spectrum immediately recovers its initial two-band pattern.

It has been widely shown (*e.g.*, Salje *et al*., 2000; Carpenter & Boffa-Ballaran, 2001; Hertwech & Libowitzky, 2002 and references therein) that structural changes occurring during a phase transition lead to changes in the phonon spectra. Such changes include peak shift, peak splitting and peak broadening; this latter feature is particularly significant in high-T spectroscopy. As a consequence, the transition temperature cannot be straightforwardly extracted from the OH-spectra given in Fig. 1. With increasing T, we actually observe two simultaneous effects: an intrinsic broadening of the two bands due to a temperature effect, and their merging due to the $P2_1/m \rightarrow C2/m$ phase transition. The combination of these two effects prevents a reliable deconvolution of the spectra if the FWHM or the peak positions is not constrained during the fitting process. In our opinion, therefore, the T of complete merging of the two components can be best located by visual inspection of the spectra, as the point beyond which there is no major change (Fig. 2). We estimate that T_c can be bracketed in this way with an uncertainty of

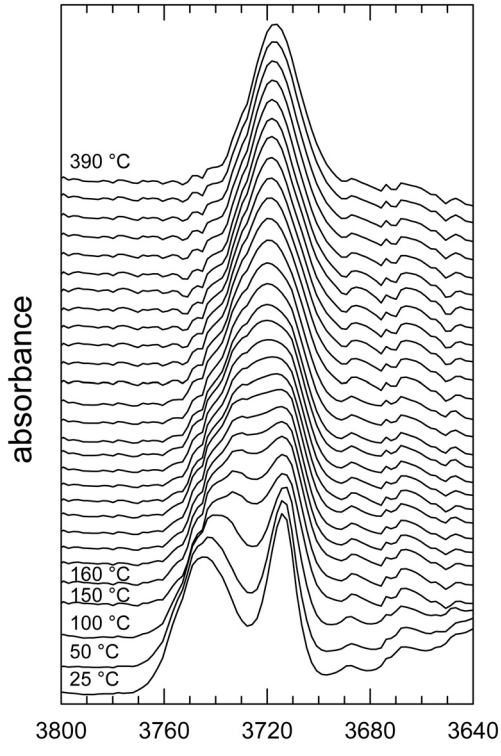

Fig. 1. Evolution of the OH-stretching region (sample 405) as a function of increasing T. From 160 °C up to 390 ° the T step is 10 °C.

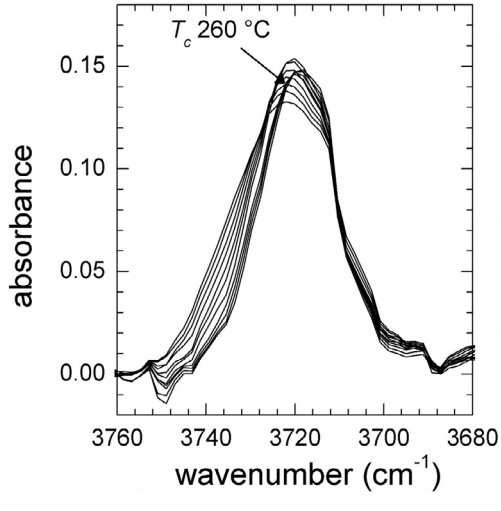

Fig. 2. Example of the "visual" estimation of the transition temperature using the OH-bands, sample 403. Note that after ~ 250 °C there are no more major changes in the spectrum.

± 10 °C (because of the step used in collecting the data), which is however reasonable for comparison (see below). A list of the transition temperatures obtained by inspection of the OH spectra is given in Table 2. Note that these values represent the highest temperature beyond which no major change in the spectra is observed.

Table 2. ifferent estimates of T_c (in °C) obtained for the studied samples using the different methods, see text for explanation.

Sample	OH-region, visual estimate*	Peak shift of the A band**	Δcorr$_{730}$ analysis
403	250(10)***	247(10)	230
405	280(10)	286(7)	270
406	320(10)	308(5)	310
407	340(10)	317(5)	320

* T beyond which there are no major changes in the spectra; ** fitting a 2-4-6 Landau potential to the variation of $\Delta\nu_A$ with T; *** for this method the uncertainty can be considered to be ± 10 °C.

High-T FTIR spectra: the MIR (1300–640 cm^{-1}) region

Figure 3 shows the typical evolution of the FTIR spectrum in the medium infrared (MIR) 1300–640 cm^{-1} region as a function of increasing T. This spectral region is poorly studied for amphiboles and for silicates in general (see Milkey, 1960, and the classical book edited by Farmer, 1974). The many bands observed in the 1200–800 cm^{-1} range can be broadly assigned to the tetrahedral T-O stretching vibrations (Ishida, 1989, 1990); the multiplicity of components observed in Fig. 3 can be explained considering the different T-O bonds occurring in the amphibole structure. The bands in the 800–650 cm^{-1} range are usually assigned to the T-O-T and O-T-O stretching and/or bending vibrations, and the OH bending (δ_{OH}) modes (Ishida, 1989, 1990). Because from a structural point of view the $P2_1/m \rightarrow C2/m$ transition in amphiboles is mainly associated with geometrical changes in the double chains of tetrahedra (see Cámara *et al*., 2003a for details), the spectra collected in the MIR region can be used to estimate the T_c, as already shown by Boffa Ballaran *et al*. (2001) in cummingtonite.

Figure 3 shows that the room-T spectrum in the 1300–820 cm^{-1} segment (segment 1) consists of overlapping bands centred at ~ 1150 (band A), 1100 (B), 1050 (C), 980 (D), 940 (E) and 915 (F) cm^{-1}, respectively. With increasing T, we observe a general broadening and a slight shift of all these bands; however, the most notable feature is the progressive merging of the two most intense components at 980 (D) and 940 (E) cm^{-1}.

At room T, the 820–640 cm^{-1} range (segment 2 in Fig. 3) also shows several absorptions: the two most prominent are centred at ~ 750 (G) and 670 (H) cm^{-1}, and a minor and broader absorption is observed at 720 (I) cm^{-1}; all bands in this range simply shift and broaden with increasing T.

Peak shift as a function of T

As already shown to be the case for cummingtonite (Boffa Ballaran *et al*., 2004), the parameter that can be determined with the highest precision in the spectral region of Fig. 3 is the wavenumber shift of the higher-frequency component A at 1140 cm^{-1}. However, the bands G and H, at ~ 750 and 670 cm^{-1} respectively, show the same type of shift.

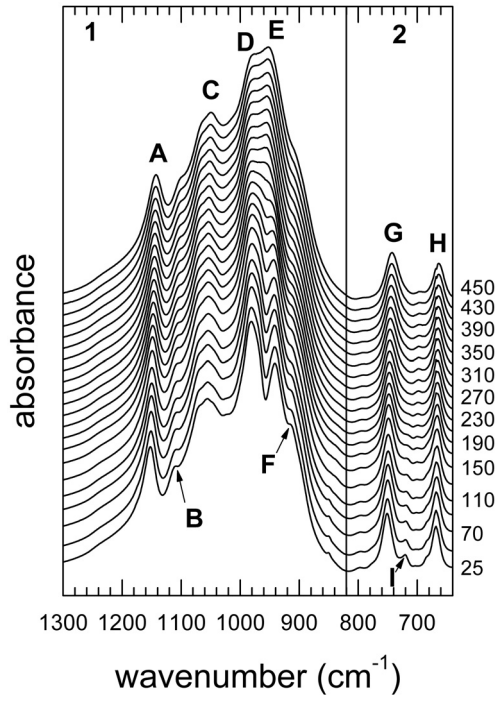

Fig. 3. Evolution of the FTIR spectra (sample 403) in the low-frequency 1300-640 cm^{-1} region as a function of increasing T; temperatures given in °C.

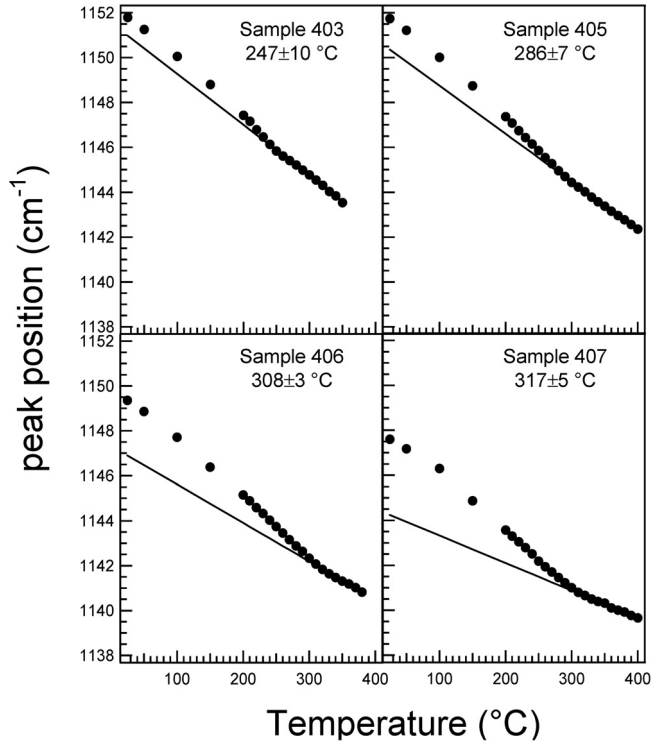

Fig. 4. Wavenumber shift of the high-frequency band A (see Fig. 3) observed as a function of increasing T for the studied samples. Lines are linear fitting to the high temperature data.

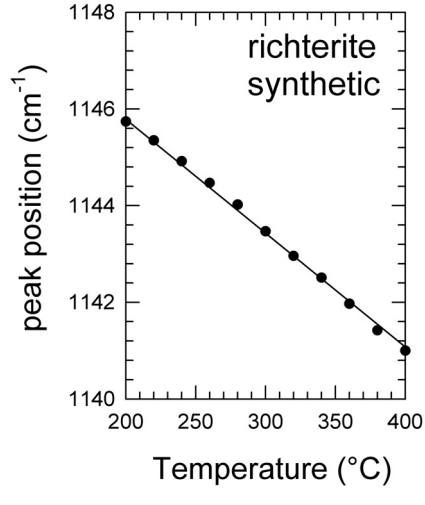

Fig. 5. Wavenumber shift as a function of T of the high-frequency A band for a richterite $[^{A}Na^{B}(NaCa)^{C}Mg_5^{T}Si_8O_{22}^{W}(OH)_2]$ synthesized by Robert *et al*. (1989).

For all spectra, the exact peak position of band A was determined by analysing the second derivative of the intensity as a function of the wavenumber; the results are given in Fig. 4 as a function of T, and are compared with the analogous plot (Fig. 5) obtained for a synthetic richterite $[^{A}Na^{B}(NaCa)^{C}Mg_5^{T}Si_8O_{22}^{W}(OH)_2]$, the amphibole with the closest composition and the same charge arrangement, which however does not undergo a $P2_1/m \rightarrow C2/m$ phase transition. Comparison of Fig. 4 and 5 shows that, unlike richterite, all the LNMSH samples of this work are characterized by a well-defined break in the peak shift of the A band, therefore the data plotted in Fig. 4 can be used to determine the $P2_1/m \rightarrow C2/m$ transition temperature for these amphiboles. Linear extrapolation of the high-T data points to room-T provides the baseline from which one can calculate the excess frequency ($\Delta\nu_A$) at each temperature of the low-T $P2_1/m$ phase. Although not very large ($< 3.5\ cm^{-1}$), the values of $\Delta\nu_A$ obtained at room-T vary for each composition, with the largest excess value observed for the ^{B}(LiMg) end-member. This feature agrees well with the larger spontaneous strain found by Iezzi *et al*. (2005) for sample 407 with respect to that determined by Cámara et al. (2003a) for a crystal with composition close to sample 403.

The $\Delta\nu_A$ value is expected to vary with the square of a short-range-order parameter associated with the displacive phase transition, *i.e.* q^2 (Bismayer, 1990; Salje & Bismayer, 1997). The variation of $\Delta\nu_A$ with T is not linear (Fig. 6), and can be fitted with a 2-4-6 Landau potential:

$$\Delta G = \frac{1}{2}a(T - T_c)q^2 + \frac{1}{4}bq^4 + \frac{1}{6}cq^6. \quad (1)$$

At equilibrium $\partial G/\partial(\Delta\nu_A) = 0$, and substituting q^2 with $\Delta\nu_A$, we can express the temperature as a function of $\Delta\nu_A$:

$$T = T_c - \frac{b}{a}\Delta\nu_A - \frac{c}{a}\Delta\nu_A^2. \quad (2)$$

The calculated transition temperatures are reported in Table 2, while the fitted ratios of Landau coefficients are reported in Table 3. Sample 407 has a c/a coefficient ratio

Table 3. Estimates of ratios of Landau coefficients obtained finding solutions to a 2-4-6 Landau potential.

Sample	b/a (°C)	c/a (°C)
403	–11 (67)	295 (80)
405	65 (25)	75 (17)
406	67 (7)	18 (5)
407	83 (9)	–1 (5)

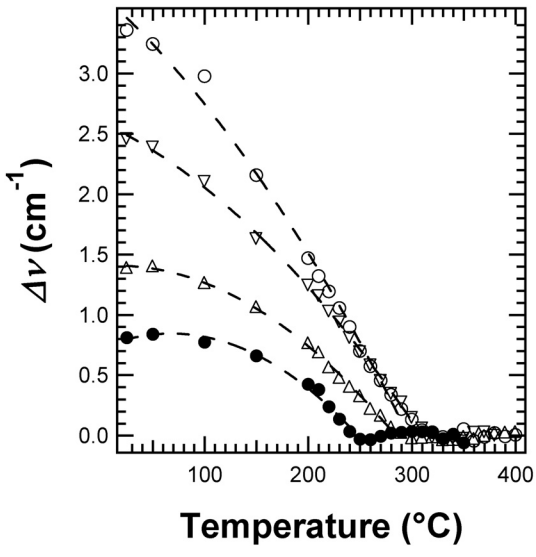

Fig. 6. Difference between the observed data and fitted baselines at high-T (see text for explanation) of the high-frequency A band for the studied compositions. Black dots = sample 403; upwards triangles = sample 405; downwards triangles = sample 406; open dots = sample 407. The dashed curves are 2-4-6 Landau potentials fits to data.

smaller than the error and is probably better fitted with a 2–4 potential (*i.e.* neglecting the q^6 term), although the results of such a fit compare well within errors (T_c = 312(6) °C and b/a = 79(2) °C). On the other hand, sample 403 has a negative and again not significant value for the b/a ratio (–11 with an estimated error of 67, *i.e.* five times larger) indicating tricritical behaviour. Fitting a 2–6 potential (*i.e.* neglecting the q^4 term) we obtain T_c = 248(8) °C and c/a = 282(20) °C, again equivalent (within the error) to the results of the 2-4-6 fitting. Therefore, in order to keep internal consistency, all data have been fitted using a 2-4-6 potential.

The same procedure has been applied to bands G and H in the low frequency region. The observed trends are similar to those of Figure 6, but the calculated $\Delta\nu_G$ and $\Delta\nu_H$ values are far below the nominal resolution of 4 cm^{-1} (< 1.6 cm^{-1} and < 0.5 cm^{-1}, respectively), and thus unsuitable for any reliable discussion.

Band broadening as a function of T

Changes in the line widths of the IR spectra occurring during a phase-transition can be conveniently modelled using the autocorrelation method (Salje *et al.*, 2000). This approach has been widely used in crystal-chemical and thermodynamic studies during the last decade (see Malcherek *et al.*, 1995; Boffa Ballaran *et al.*, 1998, 2001; Hertwech & Libowitzky, 2002 among the others). The main advantage of this method is that it does not require any assignment of the observed absorptions to their phonon modes. An additional advantage of this method is that it allows some insight into the thermodynamic character of the transition (*e.g.* Hertwech & Libowitzky, 2002).

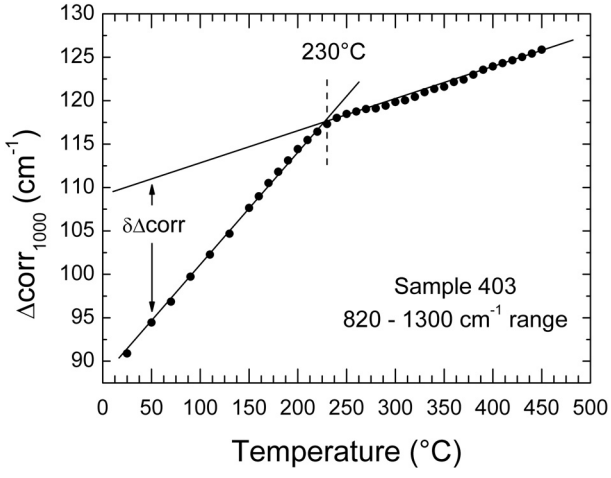

Fig. 7. Evolution of Δcorr_{1000} as a function of increasing T for sample 403.

For the samples of this work, we calculated Δ_{corr} values (see Salje *et al.*, 2000 for a detailed description of the method) for the two spectral ranges 1300-820 cm^{-1} and 820–640 cm^{-1} shown in Fig. 3.

Figure 7 shows the evolution with T of the Δcorr_{1000} calculated for sample 403 in the higher-frequency segment 1 (820–1300 cm^{-1}: the intermediate frequency 1000 cm^{-1} being used as a label). The data show a well defined break at the transition temperature, and a linear fitting of the segment above the transition yields T_c = 230 °C. Similar evolutions, although not as well defined as that shown in Fig. 7, were obtained for all the other samples. The autocorrelation of the lower-frequency segment 2 (820–640 cm^{-1}, the intermediate frequency 730 cm^{-1} being used as a label) gave more consistent results. An example of the evolution with T of the Δcorr_{730} for sample 406 is given in Fig. 8. Unfortunately, the observed evolution with T of the Δcorr values does not allow a reliable fitting using a Landau potential. Therefore, estimation of T_c has been done by finding the crossover point of the two lines obtained by fitting the high-T and low-T data. The T_c estimates obtained with this method are also given in Table 2, where comparison can be made with the values obtained using all the above described procedures.

The $P2_1/m \leftrightarrow C2/m$ phase-transition in amphiboles as a function of T

All the LNMSH amphiboles have constant composition for the A, C and T cations and the O(5) anion; the only

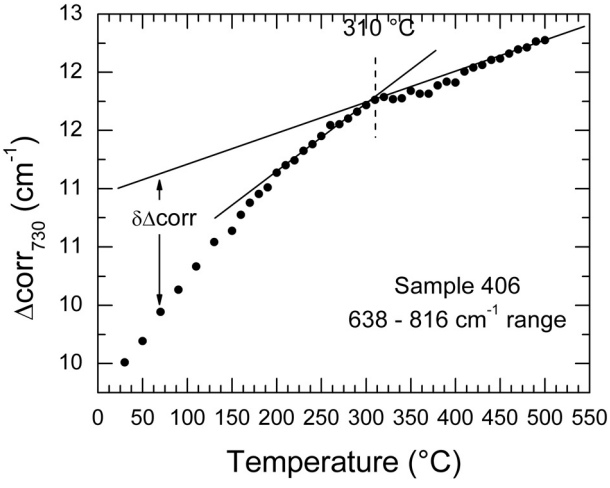

Fig. 8. Evolution of $\Delta corr_{730}$ as a function of increasing T for sample 406.

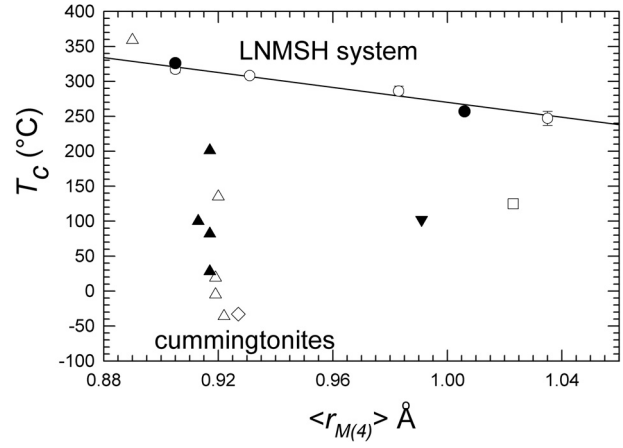

Fig. 9. Evolution of the transition temperature (T_c) as a function of the mean ionic radius of the $M(6)$ polyhedron ($\langle r_{M(6)} \rangle$). Open dots = this work; black dots = Cámara *et al*. (2003a) and Iezzi *et al*. (2005); filled downward triangle = Mn-rich parvo-tremolite (Reece *et al*., 2000); open square = Cámara *et al*. (2008); black upward triangle = annealed samples from Boffa Ballaran *et al*. (2004); open upward triangle = natural samples from Boffa Ballaran *et al*. (2004); open diamond = Yang & Smith (1996). The line is a fit to the samples of the NLMSH system, and has the equation: T_c (°C) = 803–533 $\langle r_{M(6)} \rangle$ (R^2 = 0.97).

chemical variable in this system concerns the B cations and is represented by the $^{B}Na^{B}_{-1}Li$ exchange (neglecting minor departures towards cummingtonite according to the $^{A}Na^{B}_{-1}Na^{A}_{-1}\square - {}^{B}Mg$ exchange).

Figure 9 compares the T_c calculated by fitting a Landau potential to the $\Delta\nu_A$ values for the studied samples with other T_c values from the literature plotted as a function of the aggregate ionic radius of the B cations (Shannon, 1976; given the different coordination of the various cations in the two symmetries, we used 8-fold coordination to account for the whole local environment). In the LNMSH system, T_c correlates linearly with the aggregate radius of the B cations [T_c (°C) = 803–533 $\langle r_{M(6)} \rangle$; R^2 = 0.97]. The data obtained using X-ray diffraction on samples 334 and 407 (Cámara *et al*., 2003a; and Iezzi *et al*., 2005; filled circle) fall on the same line. This behaviour is similar to what observed in cummingtonite, where the relevant exchange is $^{B}Mg^{B}_{-2}Fe_2$ (Yang & Hirschmann, 1995; Boffa Ballaran *et al*., 2004); however the trend observed for these latter samples is significantly different. Examination of Fig. 9 shows that, although for both series T_c is positively correlated with $\langle r_{M(6)} \rangle$, the slope of the $P2_1/m \leftrightarrow C2/m$ phase-boundary is different, being much steeper in cummingtonite than in LNMSH amphiboles. In other words, in cummingtonite a very small change in $\langle r_{M(6)} \rangle$ implies a greater change in T_c, and the $P2_1/m$ structure is thus far less stable than in the LNMSH system. Anyway, Fig. 9 confirms that T_c in amphibole is not a simple function of $\langle r_{M(6)} \rangle$, but that there are additional factors to consider to explain the strong difference between the two series.

In the cummingtonite series, where the *A*site is vacant, variations in B cations involve only small divalent cations (Mg, Fe, Mn) with relatively small differences in the ionic radii (0.89, 0.92 and 0.96 Å, respectively, in 8-fold coordination). In contrast, in the synthetic series investigated here, the *A* site is almost filled by Na and both monovalent and divalent B cations are present in a 1:1 ratio; the range in the ionic radius of the B cations is much wider (Mg: 0.89, Li: 0.92 Na: 1.18 Å).

There are thus three possible factors to consider in order to understand why in these compounds the slope of the regression equation is less steep than in cummingtonite: (1) the *A*-site occupancy, (2) the presence of B cations with different charges and (5) the relative values of the aggregate radii of the B and C cations. Points (1) and (2) are obviously coupled because of local constraints related to bond-strength requirements, which force ordering of the A cation close to the monovalent B cation. Point (5) can be addressed by considering the work of Cámara *et al*. (2003a, 2008), who measured a ΔT_c of + 132 °C due to the exchange of F for OH in $^{A}Na^{B}(NaMg)^{C}Mg^{T}_{5}Si_8O^{W}_{22}(OH,F)_2$. This difference can only be ascribed to point (5), and corresponds to refined $\ll M$–O$\gg$ distances of 2.077 and 2.065 Å for the OH and F end-members, respectively. Notably, the difference in $\ll M$-O$\gg$ derives only from the shrinkage of the $M(1)$ and $M(5)$ sites [coordinated to F at O(5)]. No other data are available on fluorine end-members with different mixtures of B cations; however, there is no reason to think that the trend should not be parallel to that of their OH-counterparts.

Point (5) is however also relevant in cummingtonite, where re-equilibration at higher T of a given composition allows Fe ordering at the $M(2)$ site at the expense of the $M(6)$ site (Yang & Hirschmann, 1995; Boffa Ballaran *et al*., 2001, 2002). Hence, $\langle r_{M(6)} \rangle$ decreases and $\langle r_{M(1,2,3)} \rangle$ increases more rapidly, whereas T_C increases significantly.

Sueno *et al*. (1973) first proposed that, at least at the macroscopic scale, the driving force of the $P2_1/m \leftrightarrow C2/m$ phase transition resides in the differential expansion of the various structure moduli. We want to suggest here that also the need for a local ordering of the A and monovalent B cations stabilizes the $P2_1/m$ structure: in fact, the A site can

be more strongly off-centred in the $P2_1/m$ structure, where the non-equivalence of the two double-chains of tetrahedra also allows a better coordination for both small and large B cations.

The thermodynamic character of the phase-transition

A quick inspection of the Landau coefficients reported in Table 3 shows that while the data for sample 407 can be fitted well with a 2–4 Landau potential (*i.e.* their c/a ratio is not significant), those of sample 403 are consistent with a strongly tricritical character (*i.e.* their b/a ratio is not significant); in the series, the calculated c/a value rapidly increases as a function of the $^{B}Li^{B}_{-1}Na_1$ substitution.

Differently to the thermodynamic characters inferred by infrared spectroscopy, Cámara *et al*. (2003a, 2008) in their single-crystal diffraction experiments observed a 2nd order transition for both OH and F-rich ^{B}Li-free compositions, and Iezzi *et al*. (2005) observed a tricritical character for the (OH) ^{B}Li-rich composition (sample 407) in their powder-diffraction experiments. It is relevant to the present discussion to remind that diffraction experiments yield a long-range order parameter (Q), whereas FTIR analysis yields a short-range order parameter (q) which scales with $\Delta\nu_A$. Boffa Ballaran *et al*. (2004) already noted that the variation of the ratio I_b/I_a (the normalized sum of the intensity of selected superlattice reflections, which is $\propto Q^2$) was not collinear with $\Delta\nu_A$ ($\propto q^2$), whereas the T_c values obtained by both methods were in good agreement. The same conclusion can be drawn for the samples of this work, where the T_c values obtained by FTIR spectroscopy and diffraction methods are in a very good agreement. Our results thus provide further evidence that the local structure evolves in a different manner than the crystal structure which is averaged over thousands of unit cells.

Coupling between the aggregate radius at the $M(6)$ site and the transition temperature

The Landau formalism can also be used to discuss how composition (and hence site-geometry) correlates (couples) with the occurrence of a displacive phase-transition. Boffa Ballaran *et al*. (2000), hypothesized that the value of the P_c can be renormalized by coupling of a order parameter related to the $P2_1/m \leftrightarrow C2/m$ phase-transition (Q) with composition ($X_{Fe}^{M(6)}$) and/or non convergent ordering (Q_{nco}), such as:

$$P_c^* = P_c - \frac{2\lambda_{Fe}X_{Fe}^{M(6)}}{a_v} - \frac{2\lambda_{nco}Q_{nco}}{a_v} \quad (3)$$

where, λ_{Fe} and λ_{nco} are the coupling coefficients and a_v is the Landau coefficient for the quadratic term; the dependence of the value of the critical temperature on X_{Fe} and/or Q_{nco} can be also worked out considering that Q_{nco} and Q couple through common spontaneous strain (see Cámara *et al*. 2003b for a detailed description) as:

$$T_c^* = T_c - \frac{2\lambda_{Fe}X_{Fe}^{M(6)}}{a} + \frac{2\lambda_{\varepsilon}Q_{nco}}{a} \quad (4)$$

where a is the Landau coefficient of the quadratic term of the Landau expansion and λ_s is the common strain coupling coefficient. Equation (2) implies that increasing $X_{Fe}^{M(6)}$ (and consequently increasing $\langle r_{M(6)}\rangle$) reduces the value of the effective critical temperature (T_c^*). Cation disordering (*i.e.* the migration of Fe from $M(6)$ to $M(2)$, with a shortening of $\langle r_{M(6)}\rangle$) involves a decrease of Q_{nco}; hence an increase of T_c^* is expected only if the sign of (λ_s/a) is negative. A negative sign has been indeed observed for the equivalent coupling coefficient in pigeonites by Cámara *et al*. (2003b). As a consequence, the determination of the sign of the coupling terms is essential when using equation (2) to quantify the coupling between composition and T_c. As shown in Fig. 9, there are different trends for Fe-Mg compositions with empty A sites, Mn-rich compositions with partially occupied A sites, F-rich compositions with filled A sites and OH-rich compositions with filled A sites. The compositional variation in the system studied here is simpler than in cummingtonites. As a matter of fact, we can renormalize T_c considering a compositional term related solely to the $M(6)$ site geometry, which is the only variable in this system. If we use $\langle r_{M(6)}\rangle$, T_c^* becomes:

$$T_c^* = T_c - \frac{2\lambda_{M(6)}\langle r_{M(6)}\rangle}{a}. \quad (5)$$

The equation fitted above throughout the data points [T_c (°C) = 803–533 $\langle r_{M(6)}\rangle$] implies that

$$\frac{2\lambda_{M(6)}}{a} = 533\ (\text{KÅ}^{-1}) \quad (6)$$

hence a significant coupling of the displacive transformation with $\langle r_{M(6)}\rangle$ is confirmed in the LNMSH system.

Acknowledgements: This work was funded by CNR to IGG-Unità di Pavia through the CNR-project TA01.004.002. The constructive comments of two unknown referees helped to improve the clarity of the text.

References

Bismayer, U. (1990): Hard mode Raman spectroscopy and its applications to ferroelastic and ferroelectric phase transitions. *Phase Trans*., **27**, 211-267.

Boffa Ballaran, T., Carpenter, M.A., Domeneghetti, M.C., Salje, E.K.H., Tazzoli, V. (1998): Structural mechanisms of solid solution and cation ordering in augite-jadeite pyroxenes: II. A microscopic perspective. *Am. Mineral*., **83**, 434-443.

Boffa Ballaran, T., Angel, R.J., Carpenter, M.A. (2000): High-pressure transformation behaviour of the cummingtonite-grunerite solid solution. *Eur. J. Mineral.*, **12**, 1195-1213.

Boffa Ballaran, T., Carpenter, M., Domeneghetti, M.C. (2001): Phase transition and mixing behaviour of the cummingtonite-grunerite solid solution. *Phys. Chem. Minerals*, **28**, 87-101.

Boffa Ballaran, T., McCammon, M.C., Carpenter, M. (2002): Order-parameter behavior at the structural phase transition in cummingtonite from Mössbauer spectroscopy. *Am. Mineral.*, **87**, 1490-1493.

Boffa Ballaran, T., Carpenter, M., Domeneghetti, M.C. (2004): Order parameter variation through the $C2/m - P2_1/m$ phase transition in cummingtonite. *Am. Mineral*., **89**, 1717-1727.

Cámara, F., Oberti, R., Iezzi, G., Della Ventura, G. (2003a): The $P2_1/m \leftrightarrow C2/m$phase transition in synthetic amphibole Na NaMg Mg_5 Si_8 O_{22} $(OH)_2$: Thermodynamic and crystal-chemical evaluation. *Phys. Chem. Minerals*, **30**, 570-581.

Cámara, F., Carpenter, M.A., Domeneghetti, M.C., Tazzoli, V. (2003b): Coupling between non-convergent ordering and transition temperature in the $C2/c \leftrightarrow P2_1/c$ phase transition in pigeonite. *Am. Mineral*., **88**, 1115-1128.

Cámara, F., Oberti, R., Casati, N. (2008): The $P2_1/m \leftrightarrow C2/m$ phase transition in amphiboles: new data on synthetic $Na(NaMg)Mg_5Si_8O_{22}F_2$ and the role of differential polyhedral expansion. *Z. Kristallogr.*, 223, 148-159.

Carpenter, M.A. & Boffa Ballaran, T. (2001): The influence of elastic strain heterogeneities in silicate solid solutions. EMU Notes in Mineralogy, **3**, 155-178.

Farmer, V.C. (1974): The infrared spectra of Minerals, The Mineralogical Society, London.

Gibbs, G.V., Miller, J.L., Shell, H.R. (1962): Synthetic fluor-magnesio-richterite. Am. Mineral., 47, 75-82.

Hertweck, B. & Libowitzky, E. (2002): Vibrational spectroscopy of phase transitions in leonite-type minerals. Eur. J. Mineral., 14, 1009-1017.

Iezzi, G., Della Ventura, G., Oberti, R., Cámara, F., Holtz, F. (2004): Synthesis and crystal chemistry of $Na(NaMg)Mg_5Si_8O_{22}(OH)_2$, a $P2_1/m$ amphibole. *Am. Mineral*., **89**, 640-646.

Iezzi, G., Tribaudino, M., Della Ventura, G., Nestola, G., Bellatreccia, F. (2005): High-T phase transition of synthetic $^{A}Na^{B}(LiMg)^{C}Mg_5Si_8O_{22}(OH)_2$ amphibole: an X-ray synchrotron powder diffraction and FTIR spectroscopic study. *Phys. Chem. Minerals*, **32**, 515-523.

Iezzi, G., Della Ventura, G., Tribaudino, M. (2006): Synthetic $P2_1/m$ amphiboles in the system Li_2O-Na_2O-MgO-SiO_2-H_2O (LNMSH). *Am. Mineral*., **91**, 425-429.

Ishida, K. (1989): Infrared study of manganoan alkali-calcic amphiboles. *Mineral. J*., **14**, 255-263.

Ishida, K. (1990): Infrared study of alkali amphiboles of the glaucophane-riebeckite series and their relation to chemical composition. *Mineral. J*., **15**, 147-161.

Malcherek, T., Kroll, H., Schleiter, M., Salje, E.K.H. (1995): The kinetics of the monoclinic to monoclinic phase transition in $Ba_2Al_2Ge_2O_8$–feldspar. *Phase Trans.*, **55**, 199-215.

Maresch, W.V. & Langer, K. (1976): Synthesis, lattice constants and OH-valence vibrations of an orthorhombic amphibole with excess OH in the system Li_2O-MgO-SiO_2-H_2O. *Contrib. Mineral. Petrol.*, **56**, 27-34.

Milkey, R.G. (1960): Infrared spectra of some tectosilicates. *Am. Mineral*., **45**, 990-1007.

Oberti, R., Ottolini, L., Della Ventura, G., Prella, D. (2000): Excess OH in amphiboles: a structural model obtained by combining structure refinement, complete chemical characterization, and FTIR spectroscopy. *Plinius*, **24**, 157.

Reece, J.J., Redfern, S.A.T., Welch, M.D., Henderson, C.M.B. (2000) Mn-Mg disordering in cummingtonite: a high temperature neutron powder diffraction study. *Mineral. Mag*., **64**, 255-266.

Robert, J.L., Della Ventura, G., Thauvin, J. L. (1989): The infrared OH stretching region of synthetic richterites in the system Na_2O-K_2O-CaO-MgO-SiO_2-H_2O-HF. *Eur. J. Mineral*, **1**, 203-211.

Salje, E.K.H. & Bismayer, U. (1997): Hard mode spectroscopy: the concept and applications. *Phase Trans.*, **63**, 1-75.

Salje, E.K.H., Carpenter, M.A., Malcherek, T., Boffa Ballaran, T. (2000): Autocorrelation analysis of infrared spectra from minerals. *Eur. J. Mineral*., **12**, 503-519.

Shannon, R.D. (1976): Revised effective ionic radii and systematic studies of interatomic distances in halides and chalcogenides. *Acta Cryst.*, **A32**, 751-767.

Sueno, S., Cameron, M., Papike, J.J., Prewitt, C.T. (1973): High temperature crystal chemistry of tremolite. *Am. Mineral*., **58**, 649-664.

Yang, H. & Hirschmann, M.M. (1995): Crystal structure of $P2_1/m$ ferromagnesian amphibole and the role of cation ordering and composition in the $P2_1/m \leftrightarrow C2/m$ transition in cummingtonite. *Am. Mineral*., **80**, 916-922.

Yang H. & Prewitt, C.T. (2000): Chain and layer silicate at high temperatures and pressures. *Rev. Min. Geochem.*, **41**, 211-255.

Welch, M.D., Cámara. F., Della Ventura. G., Iezzi, G. (2007): Non-ambient in situ studies of amphiboles. *Rev. Min. Geochem*., **67**, 223-260.

Received 25 January 2008
Modified version received 20 March 2008
Accepted 21 April 2008